HYTEC INCORPORATED

System Level Modeling of the SNAP Instrument and Analysis of Reaction-Wheel-Induced Jitter

Eric Ponslet
12/14/2000

	Name:	Phone & E-Mail	Signature:
Main Author:	Eric Ponslet	(505) 662-7329 ponslet@hytecinc.com	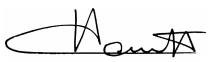
Approved:			

Abstract

A crude, system level dynamic model of SNAP is created based on the results of initial structural design studies for some of the key telescope structures. The model is used to evaluate coupled dynamics of the SNAP spacecraft with both fixed base and free-free boundary conditions to mimic launch and on-orbit situations.

The model is then used to evaluate the magnitudes of on-orbit telescope deflections induced by residual imbalances in spinning reaction wheels. It is shown that, when reaction wheel speeds are below fundamental resonances, the induced jitter is negligible or well below requirements. However, it is also found that if reaction wheel speeds are allowed to overlap structural resonances, angular mirror motions exceed requirements unless very high damping levels are present.

DESIGN ENGINEERING
ADVANCED COMPOSITE APPLICATIONS
ULTRA-STABLE PLATFORMS

110 EASTGATE DR.
LOS ALAMOS, NM 87544

PHONE 505 661-3000
FAX 505 662-5179
WWW.HYTECINC.COM

SNAP

Revision Log

Rev.	Date	Author(s)	Summary of Revisions/Comments
-	12/14/00		Initial release.

Table of Contents

1. Definitions

- FE(M): Finite Element (Model).
- DOF: Degree of Freedom.

2. System Level Dynamic Model

2.1 Assumptions, Approximations, and Point Design

A very approximate (including only key structural and optical components) system dynamics model of the SNAP spacecraft and instrument[1] was assembled in NASTRAN FE software. The model is intended to provide a first indication of the dynamics of the spacecraft-instrument assembly, uncover any unexpected couplings, and evaluate jitter induced by reaction wheel imbalance.

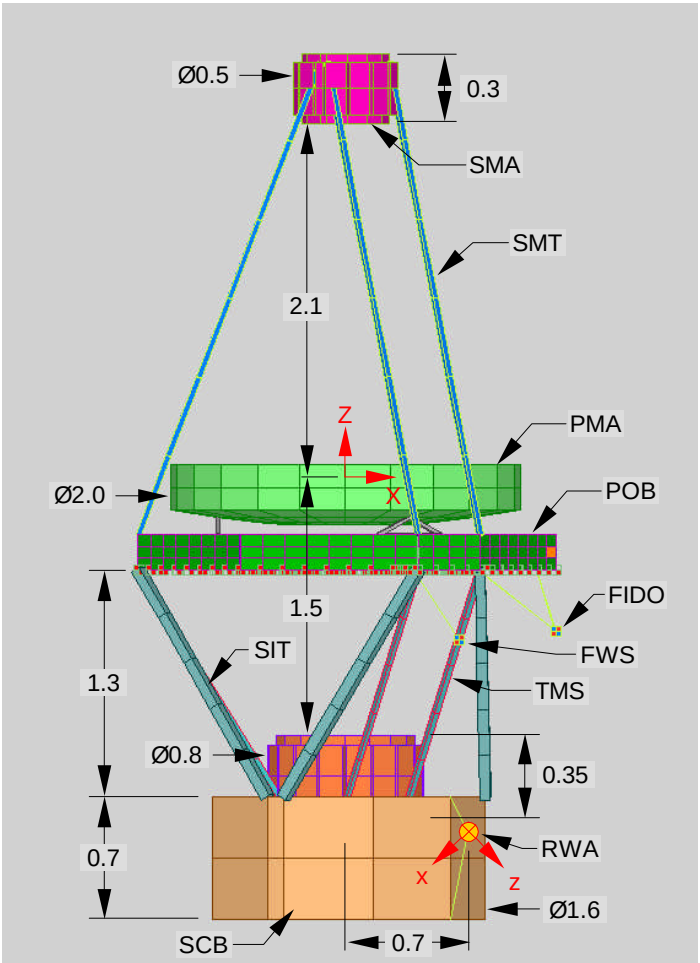

Figure 1: partial and simplified FE system model of the SNAP spacecraft; all dimensions in meters.

Subsystems for which a baseline structural design was defined were modeled as elastic bodies; those include the Primary Optics Bench[7], Primary Mirror[7], Secondary[5] and Tertiary[6] Metering Structures, and the Spacecraft-Instrument interface Truss[6]. The spacecraft and the secondary and tertiary mirror assemblies are modeled as "infinitely" rigid blocks, with overall dimensions matching expected envelopes, a uniform density, and masses of 520 kg, 22, and 40 kg, respectively (see Table 1). The Primary Baffle Assembly and the shield were not included in the model since a design baseline was not available at this time. It is expected that the mass of the baffle and shield will be of the order of 150 kg to 300 kg, or about 11 to 22% of the current model mass. Neglecting that *mass* is conservative in estimating RWA-induced jitter because by making the inertia of the instrument smaller, it increases the base motion of the metering trusses induced by imbalance forces. The *dynamics* of those structures will of course have an impact on the system dynamics, but the effect on RWA jitter will be negligible if the natural modes of the baffle and shield can be kept above 50 Hz or so.

The model's geometry (Figure 1) is loosely based on the TMA55 optical design. An exception is the position of the FIDO and FWS mass elements, which account for the presence of the optics bench and are therefore more representative of TMA56. Note that tilting the folding mirror by a few degrees (8) from its nominal 45-degree angle can bring the FIDO out of the way of the POB without altering the optical design.

Compared to previously published structural analyses of the POB, SMS, and TMS, the following design changes were made to stiffen coupled modes of the assembly:

- the primary to secondary mirror separation was reduced from 2.4 to 2.1 meter to reflect the TMA55 design.
- the POB wall thickness was increased from 4 mm to 6 mm.
- the cross sectional dimensions of the TMS and SMS support rods were increased from 23 mm OD to 30 mm OD, leaving the wall thickness unchanged at 1mm. This increases the obscuration ration due to the SMS from 3.5% to 4.6% (still below our 5% goal).

Table 1 summarizes the various components of the dynamic model, compares their mass in the model to the budgeted mass in the requirement document[1], and lists key modeling assumptions/simplifications.

	Subsystem	FEM	Budget	Baseline design	Modeling Notes
POB	primary optics bench	130	150	flat, egg crate platform with 6 mm 100 GPa GFRP walls.	detailed shell model of egg crate structure
PBA	primary baffle (around primary mirror, above and below POB)	0	150	-	not included in model
PSH	thermal shield for primary baffle	0	150	-	not included in model
PMA	primary mirror assembly (including mounts)	328	350		simplified model using solid elements; density and modulus adjusted to match dynamics of detailed model;
SMA	secondary mirror assembly (mirror, backing structure, baffles, actuators…)	22	22	-	cylindrical block of infinitely rigid solid elements with uniform density, and infinitely rigid, mass-less shell elements to provide moment anchor for metering structures.
SMS	secondary metering structure	3.5	10	near-kinematic hexapod truss[5] with tubular rods (30 mm OD, 1mm wall) of 250 GPa tailored, near zero CTE GFRP, and built-in attachments at ends.	beam elements, with built-in (6 d.o.f.) attachments to POB and SMA. Fittings not modeled.
TMA	tertiary mirror assembly (mirror, backing structure, actuators…)	40	40	-	cylindrical block of infinitely rigid solid elements with uniform density, and infinitely rigid, mass-less shell elements to provide moment anchor for metering structures.
TMS	tertiary metering structure	1.9	10	near-kinematic hexapod truss[6] with tubular rods (30 mm OD, 1mm wall) of 250 GPa tailored, near zero CTE GFRP, and built-in attachments at ends.	beam elements, with built-in (6 d.o.f.) attachments to POB and TMA. Fittings not modeled.
CBA	central baffle assembly	0	5	-	not included in model
FMA	folding mirror assembly (folding and pickup mirrors, backing structure, actuators…)	0	4	-	not included in model
FMS	folding mirror support structure	0	1	-	not included in model
FIDO	Focal plane instrument package	150	150	-	concentrated mass & inertia element attached to POB with rigid tripod; assumed 0.35 m radius of gyration
FWS	filter wheels/shutter	85	85	-	concentrated mass & inertia element attached to POB with rigid tripod; assumed 0.35 m radius of gyration
	other instruments on POB	30	30	-	distributed at bottom surface of POB model, using concentrated mass elements
SIT	spacecraft-instrument kinematic interface	29	40	6-rod aluminum alloy kinematic truss[6] (rod cross section=0.00114 m^2), with articulated/flexured end fittings.	beam elements with moment releases at connection points with POB to simulate kinematic joints. End fittings not modeled.
SCB	spacecraft bus, complete with any instrument electronics	520	520 (dry)	-	infinitely rigid block.
	TOTAL	1339	1717 (dry)		

Table 1: Summary of SNAP system model; total mass in FE model is lower than baseline largely because baffles and shield were omitted in FEM.

2.2 Fixed-Base Vibration Modes

To simulate the dynamics of the spacecraft in launch conditions, the outer edge of the base of the spacecraft bus was fixed in the model. Natural vibration modes between 0 and 60 Hz were calculated. The results are summarized in Table 1 and Figure 2.

Mode #	frequency (Hz)	description
1	18.8	overall transverse mode in XZ plane
2	19.2	same in YZ plane
3	33.1	coupled TMS and SMS truss mode in XZ plane
4	33.2	same in YZ plane
5	38.2	truss/violin mode of SMS in YZ plane
6	38.8	same in XZ plane
7	41.3	violin mode of SMS
8	42.1	local bending mode of POB due to mass of FIDO, coupled with SMS mode
9 to 26	42.7 to 49.9	various violin modes of SMS sometimes coupled with SIT violin modes
27	58.6	strongly asymmetric longitudinal breathing mode, primarily SIT and POB

Table 2: natural vibration modes of the SNAP spacecraft in fixed base (launch) conditions, in the 0 to 60 Hz band.

Note that the spacecraft was modeled as an "infinitely" rigid block. In reality, compliance of the spacecraft bus will cause the first two natural frequencies in particular to drop. Also, the masses of the primary baffle and shield structures, which was not included in the model and sits relatively high above the separation plane will further lower those natural frequencies. Given the position of the center of mass of the baffle and shield and their budgeted mass, their effect on the fundamental transverse mode is expected to be about a 10 to 20% reduction in frequency (from 19 to between 15 and 17 Hz).

This would leave at least a 50% margin on the minimum required frequency of 10 Hz for transverse modes, leaving ample margin for bus compliance (100% margin on stiffness).

Note that, in part because all subsystems were designed to 35 Hz requirements, the system level modes tend to involve more than one substructure at a time; this is particularly clear in mode #2. Modal density in the 30 to 50 Hz range is high for the same reason.

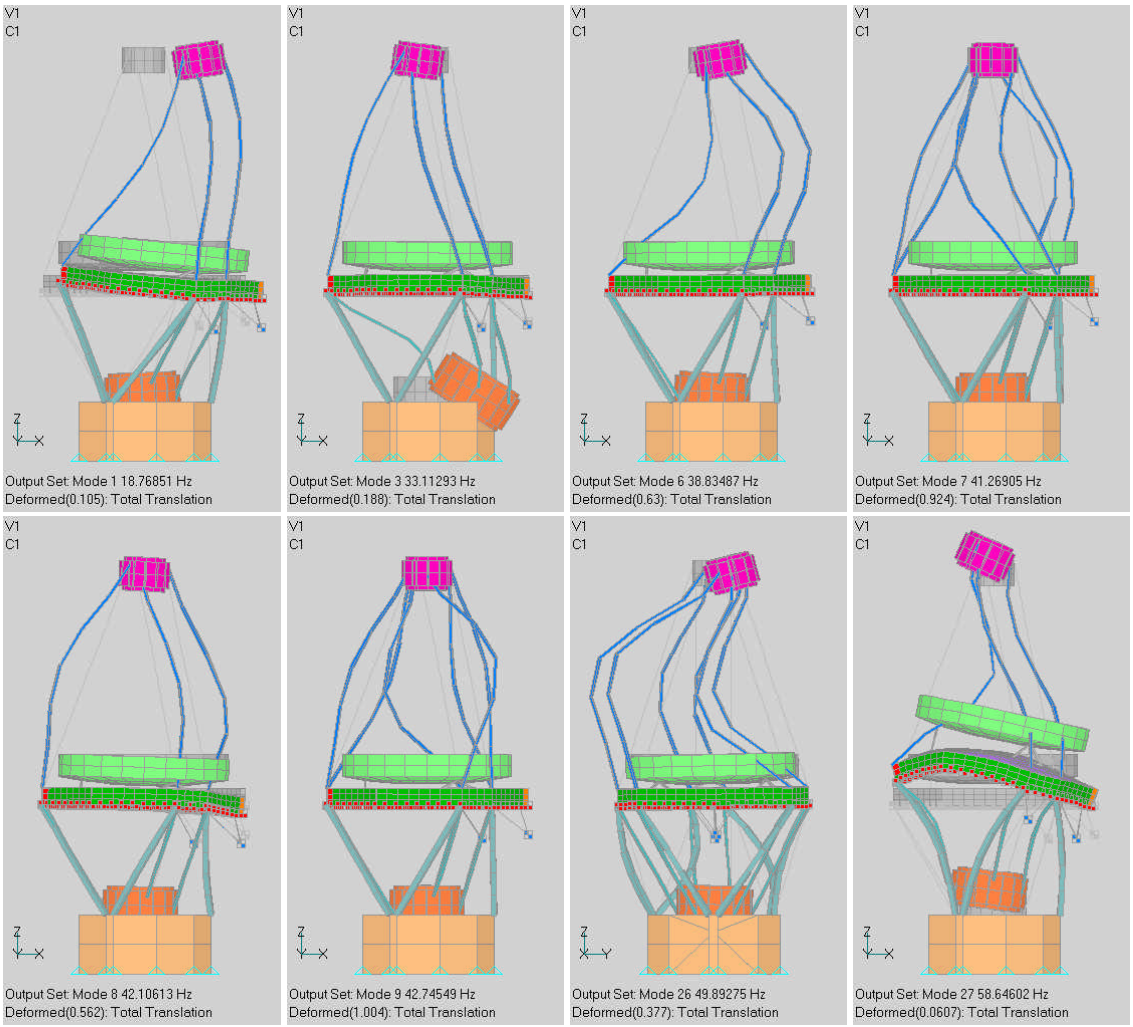

Figure 2: representative vibration modes of the SNAP spacecraft with fixed base.

2.3 Free-Free Vibration Modes

The same model was used without any boundary conditions to evaluate system dynamics in orbit conditions. Those results are summarized in Table 3 and Figure 3. The effect of neglecting spacecraft bus compliance and baffle and shield mass is smaller in this case because much smaller loads are carried in the bus and POB motion is small in most modes. Note however that since modes 7 and 27 involve more pronounced POB tilts, the effect of the baffle and shield inertia should be more pronounced on those modes.

Mode #	frequency (Hz)	description
1 to 6	0	rigid body modes
7	32.8	coupled truss mode of TMS and SMS in XZ plane
8	33.7	same in YZ plane
9	38.2	truss/violin mode of SMS in XZ plane
10	38.6	same in YZ plane
11 to 20	41.6 to 43.5	violin modes of SMS
21 to 28	46.5 to 48.2	various violin modes of SIT sometimes coupled with SMS modes
29	50.4	local bending mode of POB due to mass of FIDO, coupled with SMS mode

Table 3: natural vibration modes of the SNAP spacecraft in free-free (orbit) conditions, in the 0 to 60 Hz band.

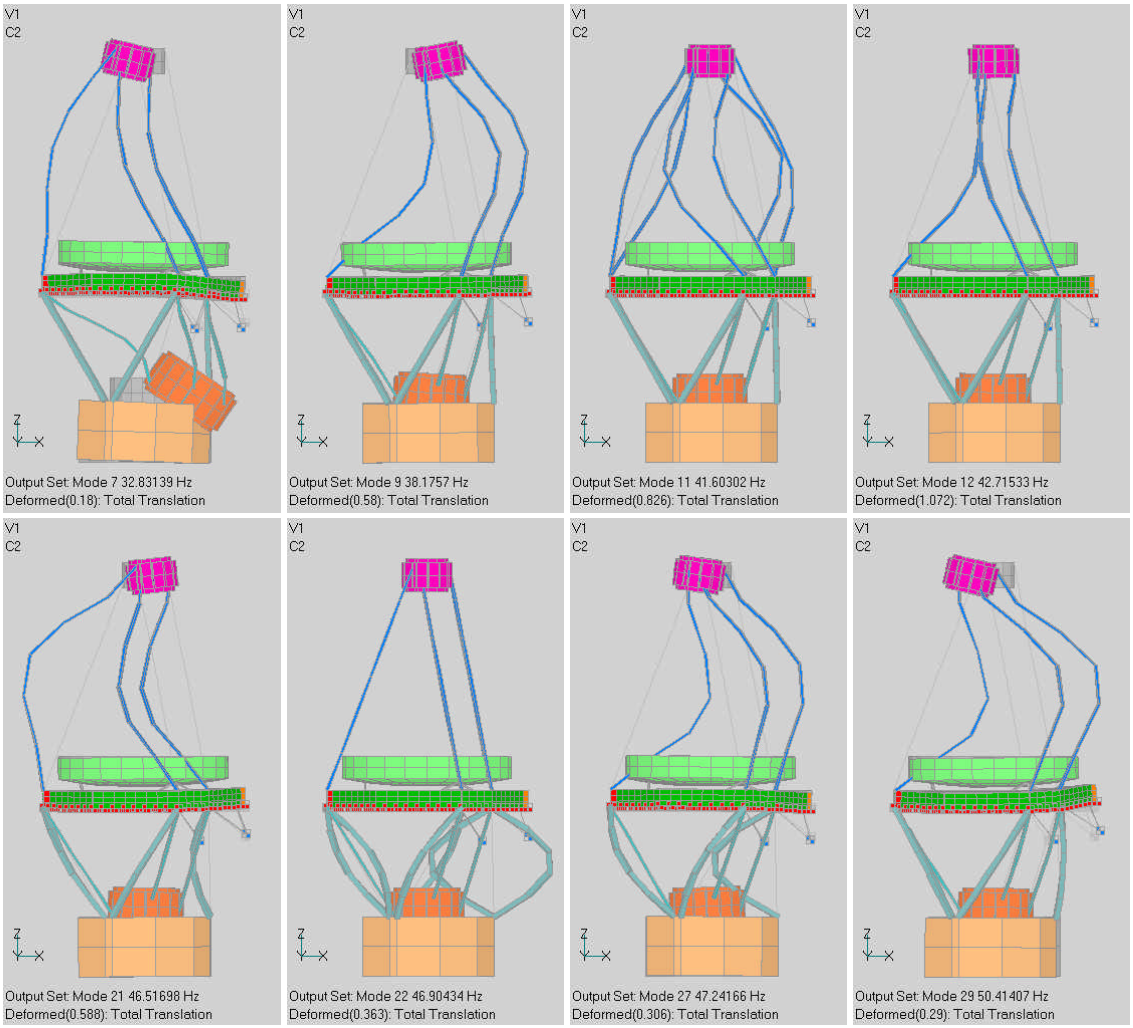

Figure 3: representative vibration modes of the SNAP spacecraft in free-free (orbit) conditions.

3. Jitter Induced by Reaction Wheel Assemblies

The main purpose for building a system model was to evaluate the amplitudes of elastic jitter caused by vibration inputs from reaction wheel imbalances. Those inputs are typically dominated by static and dynamic imbalance forces and moments that occur at frequencies equal to the rotation speed of the reaction wheels. Typical top speeds for commercially available reaction wheel assemblies are +/- 1500 to 5000 RPM (25 to 83 Hz). With free-free modes of the SNAP concept starting near 30 Hz, there is a potential for overlap between RWA excitation frequencies and major structural resonances of the telescope.

The purpose of this calculation is to determine whether such overlaps can be tolerated and in what conditions of structural damping. If overlaps cannot be tolerated, either the telescope structures must be designed more rigid, or the RPM range of the RWA's must be limited to remain below the expected fundamental frequency of the spacecraft. In considering more rigid structures, note that natural frequencies only increase as the square root of structural stiffness, and that any increase in stiffness is typically associated with some increase in mass. Because of this, even modest increases in natural frequencies may require major increases in cross sections or substantial modifications in the structural design concepts.

3.1 Assumed Reaction Wheel Arrangement for SNAP

Reaction wheel assemblies have certainly not been selected for SNAP at this stage. An initial spacecraft configuration study[4] identified the RWA15 model from L3 Communications (Figure 4) as a possible candidate. That model has relatively high moment and momentum capacities and a low top RPM speed (2200 RPM or 37 Hz). Because of the stringent stability requirements for SNAP, a micro-balanced version of that model was specified.

Spacecrafts with high performance pointing systems typically use a redundant system of four RWA, attached to the spacecraft bus, and arranged into a symmetric, four-sided pyramid. The optimum angular orientation of the spin axes relative to the spacecraft's major axis depends on the inertial properties and pointing requirements. For this study, we assumed a 45-degree angle (Figure 4).

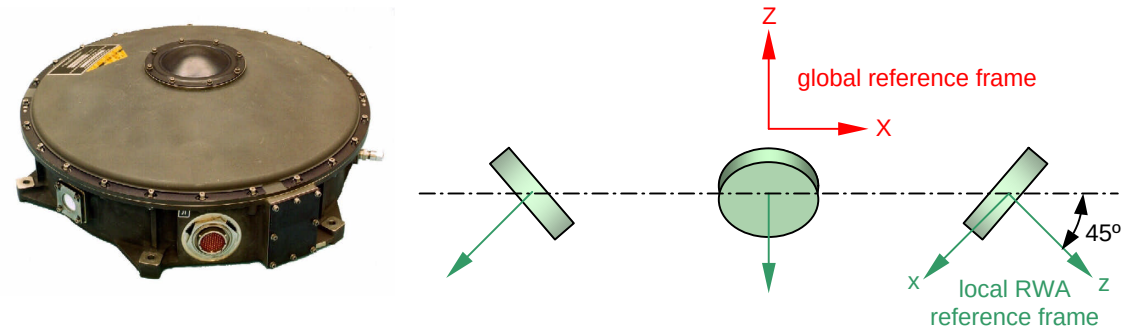

Figure 4: RWA-15 micro-balanced reaction wheel assembly from L3-Communications (left) and the assumed arrangement of four RWA's in the spacecraft bus as a 45º inverted pyramid (right).

Specifications for the RWA15 Micro-balanced system are listed in Table 4. Of particular interest to this study are the imbalance numbers. Note that effective imbalance at end-of-life (EOL) is about double the beginning of life (BOL) value. The calculations in this study are based on EOL numbers.

Feature	Value	Comments
Angular Momentum	+/- 20 Nms	
Speed Range	+/- 2200 RPM	also equal to 36.7 Hz
Reaction Torque	0.75 Nm	
Mass of rotor	5.7 kg	
Total mass	14.9 kg	
Static Imbalance	3.6×10^{-6} kg.m @ BOL	about twice as much at EOL
Dynamic Imbalance	0.92×10^{-6} kg.m^2 @ BOL	about twice as much at EOL

Table 4: Key mechanical specifications of RWA-15 micro-balanced reaction wheel assemblies from L3-Communications[2].

3.2 Modeling

3.2.1 RWA Imbalance Forces

Static and dynamic imbalances cause a rotating force f_{RWA} and moment M_{RWA} whose amplitudes are proportional to the square of the angular rate of a given RWA:

$$\left|f_{RWA}\right| = I_s\left(2pf\right)^2,$$

$$\left|M_{RWA}\right| = I_d\left(2pf\right)^2,$$

where I_s and I_d are static and dynamic imbalances, and f is the reaction wheel speed in Hz.

Phase relationship between the imbalance force and moment varies from one unit to the next. Force and moment were assumed in phase for this study. Note that other assumptions on that phase relationship could in principle have as much as a factor of 2 impact on the results. This however is within the uncertainty margins at this stage.

In orbit, all four RWAs are spinning continuously at different speeds, which result from the sequence of spacecraft maneuvers since the last reset. It is generally unlikely that two or more RWA units would be spinning at the same speed at any time. Since large structural responses are only expected at or near resonance, it is reasonable to assume that only one RWA unit will be exciting any given mode at any given time. For that reason, the modeling approach used in this study calculates the response to imbalance force and moment from *one RWA only,* as a function of its speed. Within the assumptions of this model, the response of the spacecraft to vibration inputs from all four RWA's is a superposition of four sinusoidal components at unrelated frequencies and phases.

The force and moment were modeled in NASTRAN as a set of four frequency dependent forcing terms in a local coordinate system attached to the RWA body as shown in Figure 4. The force and moment components were defined in that local frame as follows:

$$f_x = I_s (2pf)^2 \cos(2pft),$$
$$f_y = I_s (2pf)^2 \cos(2pft + \frac{p}{2}),$$
$$M_x = -I_s (2pf)^2 \cos(2pft + \frac{p}{2}),$$
$$M_y = I_s (2pf)^2 \cos(2pft).$$

Figure 5 shows the amplitude of the imbalance moment and force as a function of RWA speed (in Hz). Note that, at 30 Hz for example, the force is not negligible (0.25 N, or about 1 oz).

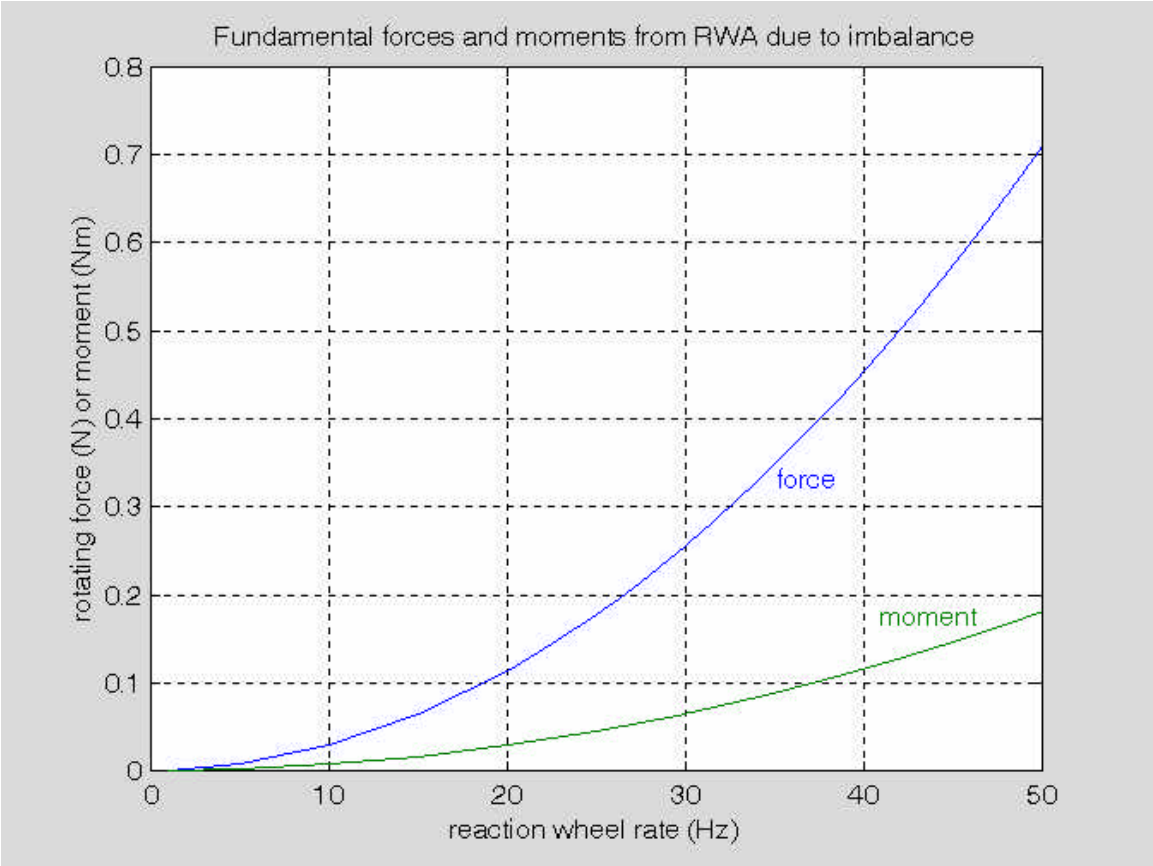

Figure 5: Amplitudes of fundamental rotating force and moment due to static and dynamic imbalance of reaction wheels, as a function of reaction wheel speed (in Hz).

Note also that in reality the actual vibration caused by a RWA is not limited to a pure sinusoidal imbalance but covers a wide frequency band with multiple harmonics and wide band noise. However, the amplitude of those harmonics and noises are typically much lower than the imbalance fundamental. In addition, any high frequency noise (above 50 Hz or so) can be effectively isolated for the spacecraft with the use of simple elastomeric mounts.

3.2.2 Structural Damping

The model is used to calculate the steady-state response of the structures to imbalance forces and moments, as a function of the wheel speed. When the wheel speed matches a resonance of the structure, the response reaches a maximum. The amplitude of the resonant response is inversely proportional to the amount of structural damping, or directly proportional to the *Q* of the mode. In very low amplitude vibrations of high stiffness precision structures, stick-slip mechanisms cannot contribute to damping. Without specifically designed damping treatments, the effective *Q* can then be very large (*Q*'s of 100 to 1000 are entirely possible).

It is difficult to estimate the likely *Q* of the SNAP structures at this stage. An arbitrary value of *Q*=100 was used in the calculations. Larger Q's would simply produce even sharper resonant peaks of proportionally larger amplitude.

3.2.3 Performance measures

SNAP requirement documents[1,3] give allowable values for the motions of the secondary and tertiary mirror at frequencies above 5 Hz. To evaluate the design against those requirements, multi-point equations were implemented in NASTRAN to calculate relative motions of the secondary and tertiary mirrors relative to the primary.

Note that mirror compliance does not affect the results in the 0 to 50 Hz frequency range. The baseline primary mirror[7] has a fundamental frequency around 333Hz. The secondary and tertiary mirror baselines use the same technology, so in view of their much smaller dimensions, their fundamental frequencies should be in the several hundreds of Hz.

3.3 Results

Figure 6 and Figure 7 show the response of the secondary and tertiary mirrors (relative to the primary) as a function of the RWA speed (in Hz), for a *Q* of 100 in all modes. Three components are shown in the figures: despace (ÄZ), and tilts in two directions ($ÄR_X$ and $ÄR_Y$). Allowable values for some components are also shown, as well as then nominal top speed to the L3Com RWA15 units.

A number of observations can be made about those results. First, only angular motions of the mirrors are significant: despace motions never exceed 3 nanometers between 0 and 50 Hz. Second, resonant responses tend to exceed allowable motions for Q's larger than 100.

Three approaches could be considered to address this last point: either avoid any overlap between RWA speeds and structural resonances, or increase the damping levels in the lower frequency modes, or attenuate transmission of imbalance forces into the bus by using isolation mounts for the RWA's.

The first approach can be achieved either by designing the structures rigid enough to push structural resonances well above the top speed of the RWA (i.e. design all structures to fundamental frequencies greater than about 50 Hz if using L3Com RWA15 models), or hold RWA speeds below structural resonance frequencies (by selecting slower models or limiting the speed range of existing models). Note that increasing the fundamental frequency of the current concept from about 30 Hz to 50 Hz requires an almost 3-fold increase in the stiffness of the key structural elements such as optics bench and metering trusses, even assuming no change in mass. Limiting the RWA top speeds to around 25 Hz may be a more palatable alternative.

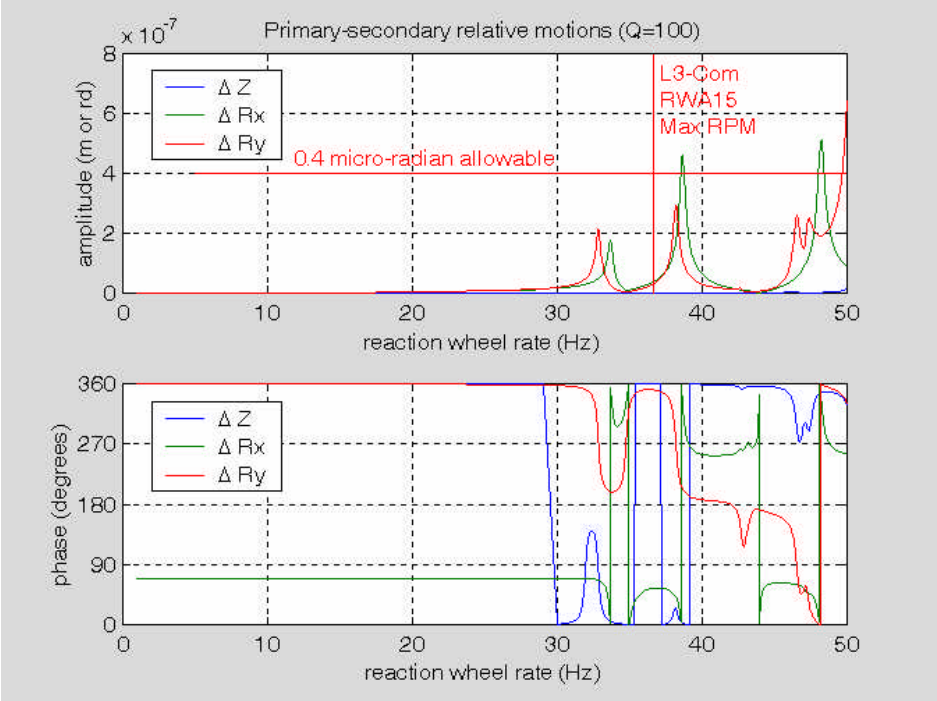

Figure 6: Relative motion of primary-secondary mirror pair induced by reaction wheel imbalance as a function of reaction wheel speed (in Hz).

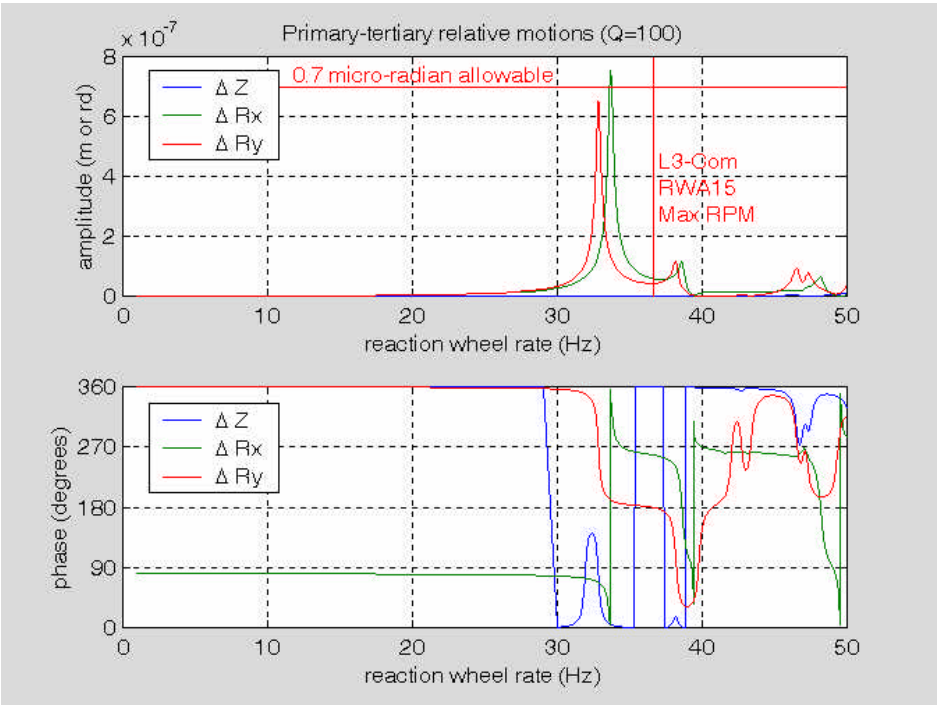

Figure 7: Relative motion of primary-tertiary mirror pair induced by reaction wheel imbalance as a function of reaction wheel speed (in Hz).

Figure 8 shows that in theory, decreasing the Q to about 10 would provide better than 500% margin between expected and allowable mirror motions. It must be noted however that, with the current baseline design, large mirror motions occur in the response of *primary* structural modes (as opposed to secondary modes such as violin modes) with most of their strain energy in primary structural elements such as the POB and the longitudinal stiffness of the metering struts. Increasing the damping levels in those primary modes to a *Q* of 10 may not be a realistic expectation, although tuned vibration absorbers may be an option worth examining.

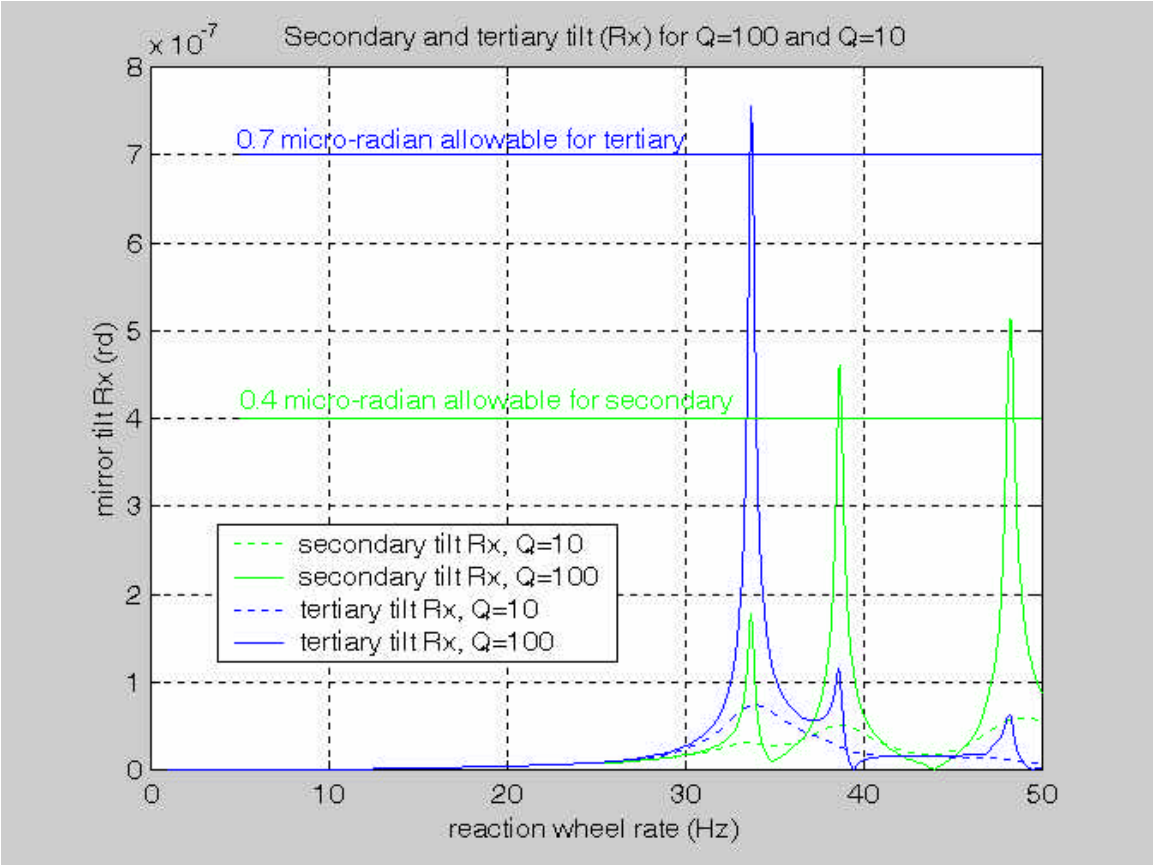

Figure 8: Relative motion amplitudes of primary-tertiary and primary-secondary mirror pairs induced by reaction wheel imbalance as a function of reaction wheel speed (in Hz); comparison of low (Q=100) and high (Q=10) damping cases.

Attenuating RWA disturbances with isolation mounts is a third option. Simple, commercially available "rubber" isolators can provide significant isolation of frequencies above 60 Hz or so, eliminating concern about higher harmonics. The isolation frequencies for a well designed 6 dof isolation system using "rubber" isolators could be about 15 to 20Hz. A single stage passive isolator will provide near 40dB/decade of isolation above its isolation frequency, so one might expect 20dB at about 65 Hz, and 40 dB around 200 Hz, and so on. It is also clear that passive isolation will not be very effective in isolating fundamental imbalance perturbations up to 30 Hz. More effective isolation of low frequencies would require extremely soft isolators which would then negatively affect the ACS control stability. A viable but expensive option is to use

active isolation platforms for the RWA's. Such platforms typically use a actuated hexapod configuration and feedback control to attenuate low frequency disturbances while maintaining a high DC stiffness. Interactions with the ACS must be considered carefully in designing control laws for such platforms. To summarize, it is clear that, at a minimum, a relatively stiff passive isolation is indicated to alleviate concerns about higher harmonics. More effective isolation (softer or active) may be considered but would require careful design with consideration of gyroscopic effects and interactions wiuth the ACS.

4. Concluding Remarks

A crude system model of the SNAP spacecraft was created to evaluate the amplitudes of mirror jitter caused by reaction wheel vibrations. Assuming moderately low structural damping (Q's of 100), the model predicts that if the reaction wheel speeds are allowed to overlap structural resonances, angular motions of the mirror will likely exceed allowable values.

Reducing jitter to acceptable levels will likely require a combination of stiffening primary structures as much as possible within obscuration and mass constraints, limiting reaction wheel top speeds well below fundamental structural modes, and possibly implementing vibration damping technology such as tuned vibration absorbers.

In addition, mounting reaction wheel assemblies on simple passive isolation mounts is recommended to eliminate any concern about jitter induced by higher harmonics of reaction wheel vibration.

5. References

1. E. Ponslet, "Design Requirements for the SNAP Telescope Structures," HTN-113005-0001-B, HYTEC, Inc., December 12, 2000.
2. Gary Gonska, L3 Communications, private phone conversation, November 14, 2000.
3. Optical Telescope Assembly Definition and Requirements Document for the Supernova / Acceleration Probe (SNAP), Draft 0.1, U.C. Berkeley and L.B.N.L, September 5, 2000.
4. H. Heetderks, "Spacecraft Design and Mission Operations", Presented to the SAGENAP review by M. Lampton, March 29, 2000.
5. E. Ponslet, "Trade Studies for SNAP Secondary Metering Structure" HTN-113005-0005, HYTEC, Inc., August 10, 2000.
6. E. Ponslet, "Initial Sizing Studies for Tertiary Metring and Spacecraft-Instrument Interface Trusses" HTN-113005-0004, HYTEC, Inc., September 12, 2000.
7. E. Ponslet, "Structural Engineering For the SNAP Telescope: Status Report," HPS-113005-0001, HYTEC, Inc., presentation to LBNL SNAP team, November 3, 2000.